Differential Mechanisms Underlying the Modulation of Delayed-Rectifier K + Channel in Mouse Neocortical Neurons by Nitric Oxide

Nian-Lin R. Han, Jian-Shan Ye, Albert Cheung Hoi Yu and Fwu-Shan Sheu

J Neurophysiol 95:2167-2178, 2006. First published Jan 18, 2006; doi:10.1152/jn.01185.2004

J Neurophysiol 95: 2167–2178, 2006.
First published January 18, 2006; doi:10.1152/jn.01185.2004.

Differential Mechanisms Underlying the Modulation of Delayed-Rectifier K^+ Channel in Mouse Neocortical Neurons by Nitric Oxide

Nian-Lin R. Han,[1] Jian-Shan Ye,[1] Albert Cheung Hoi Yu,[2] and Fwu-Shan Sheu[1,3]

[1]*Department of Biological Sciences, National University of Singapore, Singapore;* [2]*Neuroscience Research Institute, Peking University and Department of Neurobiology, Peking University Health Science Center, Beijing, China; and* [3]*The University Scholars Programme, National University of Singapore, Singapore*

Submitted 17 November 2004; accepted in final form 12 January 2006

Han, Nian-Lin R., Jian-Shan Ye, Albert Cheung Hoi Yu, and Fwu-Shan Sheu. Differential mechanisms underlying the modulation of delayed-rectifier K^+ channel in mouse neocortical neurons by nitric oxide. *J Neurophysiol* 95: 2167–2178, 2006. First published January 18, 2006; doi:10.1152/jn.01185.2004. The modulatory effects of nitric oxide (NO) on voltage-dependent K^+ channels are intricate. In our present study, the augmentation and reduction of K^+ currents by NO donor *S*-nitro-*N*-acetylpenicillamine (SNAP) and pure dissolved NO was observed in dissociated neurons from mice neocortex with both whole cell and cell-attached patch clamp. By using a specific electrochemical sensor, the critical concentrations of NO that increased or reduced the channel activities were accurately quantified. Low concentrations of SNAP (20 μM) or NO solution (0.1 μM) enhanced whole cell delayed rectifier K^+-current (I_K) and left the fast inactivating A current (I_A) unchanged. However, high concentrations of SNAP (100 μM) and NO (0.5 μM) reduced both I_K and I_A currents. In cell-attached experiments, a significant increase in channel open probability (NP_0) was observed when using low concentrations of SNAP or NO. High concentrations of SNAP or NO dramatically decreased NP_0. The increase in channel activities by low concentrations of SNAP was abolished in the presence of either inhibitors of soluble guaylate cyclase or inhibitors of cGMP-dependent protein kinase G, suggesting a link to the NO-cGMP signaling cascade. The reduction of channel activities by high concentrations of SNAP was reversed by the reducing agent dithiothreitol, implying a redox reaction mechanism. Thus both NO-cGMP signaling and a redox mechanism are involved in the modulation of I_K channel activity for neuron excitability.

INTRODUCTION

Nitric oxide (NO) has been linked to numerous important functions in the CNS, including neurotransmitter release, synaptic plasticity, and, more broadly, the modulation of neuronal electrical activity (Bredt and Snyder 1994; Ko and Kelly 1999; Stamler et al. 1997). NO is produced by nitric oxide synthase (NOS), the neuronal form (nNOS), which is activated by Ca^{2+} through calmodulin. nNOS-containing neurons are present in many areas of the CNS. Although nNOS neurons represent only roughly 1% of cell bodies in the cerebral cortex, virtually every neuron in the cortex is exposed to nNOS nerve terminals (Bredt et al. 1990; Salter et al. 1991). NO has been proposed as a retrograde messenger that coordinates the enhancement of both pre- and postsynaptic mechanisms involved in synaptic plasticity (Prast and Phillipu 2001). The actions of NO are a consequence of its influence on a variety of protein functions. It is well established that NO can exert its biological effects through the activation of guanylyl cyclase and the production of cGMP or through cGMP-independent mechanisms known as "redox signaling" (Stamler 1994). However, relatively few targets of the action of NO in neurons that could explain its role in CNS function have been identified.

K^+ channels are widely expressed throughout the brain. They play a key role in membrane potential maintenance, neuronal excitability, and synaptic transmission. The properties of many K^+ channels can be modulated through second-messenger pathways activated by neurotransmitters and other stimuli (Hille 1992; Levitan 1988). It has been shown that NO regulates several types of K^+ channels, including ATP-dependent K^+ channels and Ca^{2+}-activated K^+ channels, in both peripheral tissues and the CNS (Prast and Phillipu 2001). However, the biological mechanisms by which NO acts on the delayed-rectifier K^+ channels, especially in the CNS, are not fully understood. Delayed-rectifier K^+ channels (I_K) have been found to contribute to the repolarization of membrane potentials following action potentials, and the modulation of spike discharge in many neurons. Different NO donors or caged NO exert diverse reactions on K^+ channels, probably due to the dosages of NO or different regions of the CNS (Lang and Watson 1998; Prast and Phillipu 2001). Furthermore, both cGMP-dependent and -independent signaling pathways have been reported to involve in the modulation of Ca^{2+}-activated K^+ channel by NO (Bolotina et al. 1994; Klyachko et al. 2001; Zhou et al. 1996). The controversy of regulatory mechanism for NO on K^+ channel activity may be resolved if sensitive, quantitative detection methods are developed to measure and distinguish NO derived from various NO donors (sources) in different in situ experimental systems. In the present study, we have developed an electrochemical NO sensor that can accurately evaluate the concentration of NO released from NO donors. This study aims to address effects of NO and its effective concentrations in regulating delayed-rectifier K^+ channels, using a combination of patch-clamp electrophysiology and electrochemical NO sensor. We report here that different concentrations of NO either augment or block the delayed-rectifier K^+ channel via a dual cGMP- and redox-dependent mechanism in mouse cerebral neocortical neurons.

Address for reprint requests and other correspondence: F.-S. Sheu, Dept. of Biological Sciences, National University of Singapore, 14 Science Dr. 4, Singapore 117543, Singapore (E-mail: dbssfs@nus.edu.sg).

The costs of publication of this article were defrayed in part by the payment of page charges. The article must therefore be hereby marked "*advertisement*" in accordance with 18 U.S.C. Section 1734 solely to indicate this fact.

METHODS

Preparation of mouse neocortical neurons

All experiments were performed using primary culture of mouse neocortical neurons. Cortices were obtained from 1-day-old postnatal Tac:Icr:Ha(ICR)fBR mice as described previously (Baughman et al. 1991; Goslin and Banker 1991). In brief, cortices were dissected from the brains under sterile conditions and were digested in 0.25% trypsin in Hank's balanced salt solution (HBSS) for 20 min at 37°C. Trypsin digestion was terminated by adding 10% fetal bovine serum (FBS) and then the tissue was triturated with a plastic pipette. After centrifugation for 5 min at 200 *g*, cell pellets were mechanically dissociated by triturating in culture medium (Eagle's minimal essential medium supplemented with 10% fetal calf serum, and 2 mM glutamine) until no cell clumps could be seen. After filtering through 70 μM nylon mesh (Millipore), the cells were seeded at a density of 2.5×10^5 cells/cm^2 in 35-mm petri dishes containing circular 10-mm diameter poly-D-lysine (12.5 μg/ml)-coated coverslips. Cultures were maintained in a humidified CO_2 incubator (5% CO_2, 37°C). After 16–18 h, culture medium was changed with fresh culture medium. One day later, half of the medium was replaced with fresh medium, and 10 μM cytosine arabinoside was added to inhibit proliferation of nonneuronal cells. The cells were used for experiments for ≤7 days. All recordings were made from cells cultured between days 4 and 7.

All animal experiments were approved by the Research Committee of the University Animal Holding Unit, National University of Singapore. All efforts were made to minimize animal suffering and to reduce the number of animal used.

Electrophysiological recording

All electrophysiological experiments were carried out at room temperature (22–24°C). Voltage-clamp recordings were made from cultured neocortical neurons using standard patch-clamp methods in the whole cell and cell-attached configurations. Currents were recorded using an EPC-9 amplifier (Heka Elektronik). Data acquisition was controlled by PULSE 8.63 (Heka Elektronik). Currents were filtered at 1–2 kHz and digitalized directly to a Macintosh Power Mac G4. Data were analyzed using PULSE-Fit (Heka Elektronik) and Igor-Pro (WaveMetrics, Lake Oswego, OR).

Patch pipettes were made from 1.5-mm borosilicate capillary glass (World Precision Instruments, Sarasota, FL) using a Sutter P-97 puller (Sutter Instrument, Novato, CA). The pipettes were fire-polished and tip resistance was 2–6 MΩ for whole cell and 12–17 MΩ for single-channel recordings when filled with pipette solution (for contents, see following text).

For the whole cell recordings, the bath solution contained (in mM) 140 NaCl, 10 KCl, 2 $CaCl_2$, 1 $MgCl_2$, 10 HEPES, 2 $CdCl_2$, 10 glucose, and 0.001 tetrodotoxin (TTX) at pH 7.4. The pipette solution was composed of (in mM) 10 NaCl, 140 K-gluconate, 0.1 $CaCl_2$, 4 $MgCl_2$, 10 HEPES, and 1 EGTA at pH 7.4. At the beginning of each experiment, junction potential between pipette solution and bath solution was electronically adjusted to zero. No leakage subtraction was performed to the original recordings, and all cells with visible changes in leakage currents during the course of experiment were excluded from further analysis. Test pulses were made at 10-mV increments from −60 to +80 mV with the holding potential at −50 mV unless stated otherwise. Cells were continuously perfused with the bath solution containing test chemicals. All solutions were adjusted with osmolarity of 300 mosM/l and pH 7.4. Serial resistance (R_s) and capacity transients were electronically compensated. The mean whole-patch capacitance was 15.6 ± 7.8 pF (n = 68) and the mean R_s was 1.18 ± 0.12 MΩ. R_s compensation of 80–90% was used, with a lag of 10 μs, and was periodically checked during the experiment.

For the cell-attached recordings, both pipette and bath solution containing 140 mM KCl and 5 mM NaCl. R_s compensation was not used. Patches (seal resistance: 5–15 GΩ) were obtained on the soma of neurons. Data were analyzed using software TAC 4.02 (Bruxton, Seattle, WA). The channel open probability (P_o) was calculated from the ratio between the open time and the total time. NP_o was determined from data samples of a 60-s duration and defined as: $NP_o = \Sigma (t_1 + 2t_2 + 3t_3 + \ldots + nt_n)$, where n is channel number, and t_1, t_2, and t_n are the ratios of open time to total time for each channel at each current levels. The unit amplitude of channels and channel open duration were determined from all point histograms with a Gaussian curve. A current level higher than 50% of the unit channel current was considered to reflect a channel opening.

Measurement of NO release by SNAP using electrochemical sensor

Preparation of a saturated NO solution involves the meticulous exclusion of O_2 as NO can be oxidized rapidly by O_2 when its concentration is higher than a certain threshold. To produce a saturated NO solution free of O_2, phosphate buffer solution (PBS) at pH 7.4 was first purged with pure nitrogen gas (99.9%, Soxal) for 30 min. The O_2-free PBS buffer was then purged with pure NO gas (99.9%, Matheson) for 30 min and kept under an NO atmosphere until use. The saturated aqueous NO solution contained ~2.0 mM NO at 25°C at P_{NO} = 1 atm (Lantoine et al. 1995). The diluted NO standards were made freshly for each experiment using O_2-free, NO-saturated PBS that was kept in a glass flask with an air-tight rubber septum.

To measure NO release from the dissolved *S*-nitro-*N*-acetylpenicillamine (SNAP) in bath solution, we used a gold (Au) electrode of 2.0-mm diam (EG&G) prepared by polishing with aqueous slurries of fine alumina power (0.06 μm) on a polishing microcloth (Bioanalytical Systems) and was sonicated for 10 min in water. The electrode was then cleaned electrochemically in 0.02 M H_2SO_4 by potential cycling (CHI660A, CH Instruments, Austin, TX) across a range of −0.1 to +1.5 V at 10 V/s for 30 cycles. The pretreated Au electrode was dipped into 0.5% Nafion/ethanol solution for 5 s and then dried in air. This dipping was repeated three times. The resulting electrode is denoted as Nafion@Au.

All electrochemical measurements were performed on a BAS 100 B/W workstation (Bioanalytical Systems) controlled by the BAS 100 B/W software from a Gateway 2000 personal computer. The three-electrode system consisted of a Nafion@Au as the working electrode, an Ag/AgCl reference electrode, and a platinum wire auxiliary electrode. All potentials were quoted with respect to the reference. Prior to each measurement, the working electrode (Nafion@Au) was inserted in a solution containing 5.0 ml PBS buffer, and its potential was cycled between 0 and +800 mV at a rate of 50 mV/s until a steady response was obtained. The detection of NO was conducted in chronoamperometric mode and the solution was stirred mechanically during the experiment. The currents from the electrocatalytic oxidation of NO were recorded at the applied potential of +800 mV for monitoring the release of NO from SNAP (Bedioui et al. 1994; Do and Wu 2001; Miao et al. 2000).

Materials

All chemicals were obtained from Sigma-Aldrich (St. Louis, MO), except tetraethylammonium chloride (TEA), SNAP, *N*-[2-(methylamino)ethyl]-5-isoquinolinesulfonamide (H-8), and methylene blue (MB) from Calbiochem (La Jolla, CA). NO gas was purchased from Matheson Tri-Gas (Newark, CA). All cell culture reagents were purchased from GIBCO-Invitrogen (Grand Island, NY).

Data analysis

Results were expressed as means ± SE from at least three independent experiments. Statistical significance was determined by one-way ANOVA and the Student-Newman-Keuls post hoc test (SPSS for

Windows, SPS, Chicago, IL) for unpaired data, with $P < 0.05$ representing significance. The normalized conductances were fitted to a least squares criterion procedure with the Boltzmann function

$$G/G_{max} = (1/\{1 + \exp[-(V - V_{1/2})/k]\})^n$$

Where G/G_{max} is the conductance normalized to its maximal value, V is the membrane potential, $V_{1/2}$ is the voltage at which the conductance is half-maximal (for a single gate, $n = 1$) and k is the slope factor.

RESULTS

Properties of voltage-dependent K^+ channel of neocortical neurons

It has been previously shown that voltage-dependent K^+ currents can be separated by their current kinetics and inactivation properties (Surmeier et al. 1994). In neocortical neurons, depolarization from −120 mV activates a rapidly inactivating A current (I_A) and a delayed rectifier current (I_K); depolarization from a more positive holding potential (−50 mV) activates only the I_K because the I_A was almost completely inactivated at this potential (Hamill et al. 1991; Storm 1990).

Figure 1, *A* and *B*, shows typical currents recorded under voltage clamp in a whole cell patch from a neocortical neuron in control bath solution. The bath solution contained 0.001 mM TTX to block voltage-gated Na^+ channels and 2 mM Cd^{2+} to block voltage-gated Ca^{2+} channels and Ca^{2+}-dependent K^+ currents. The Cl^- was replaced by gluconate$^-$ to eliminate the Cl^- current. Two types of outward currents were observed. Following a range of depolarizing steps from −60 to +50 mV, the evoked currents showed the delay rectifier type of K^+ currents (I_K; Fig. 1*A*). This was further confirmed pharmacologically by adding of 10 mM TEA to the bath solution that blocked 75.6 ± 9.5% of the currents (Fig. 1*C*). When a 600-ms, −120-mV conditioning pulse was applied, a rapidly inactivating A current (I_A) occurred (Fig. 1*B*). However, the I_A current was not prominent, and only 7 in 30 cells measured showed I_A current under the voltage protocols as shown in Fig. 1. Most cells, 21 in 30 cells measured, displayed delayed rectifier type of K^+ current even the −120-mV conditioning pulse was applied. Addition of 10 mM TEA to the bath solution reduced slowly decaying current, leaving the fast component more prominent (Fig. 1*D*). The I_A current could be isolated by subtracting the current evoked by a step depolarization at a holding potential of −50 mV from those evoked from −120 mV (Fig. 1*E*).

The normalized average peak conductances, calculated by dividing the maximal current amplitude at each command voltage by the driving force calculated from the Nernst equation, were fitted with a least-squares criterion procedure with the Boltzmann function defined in *Data analysis* (Fig. 1*F*). Both the I_K and I_A currents showed voltage-dependent increase of conductances.

Low concentration of NO donor SNAP and pure NO increase the whole cell I_K current

The application of freshly prepared 20 μM SNAP to cells, held at −50 mV, resulted in a reversible increase in the whole

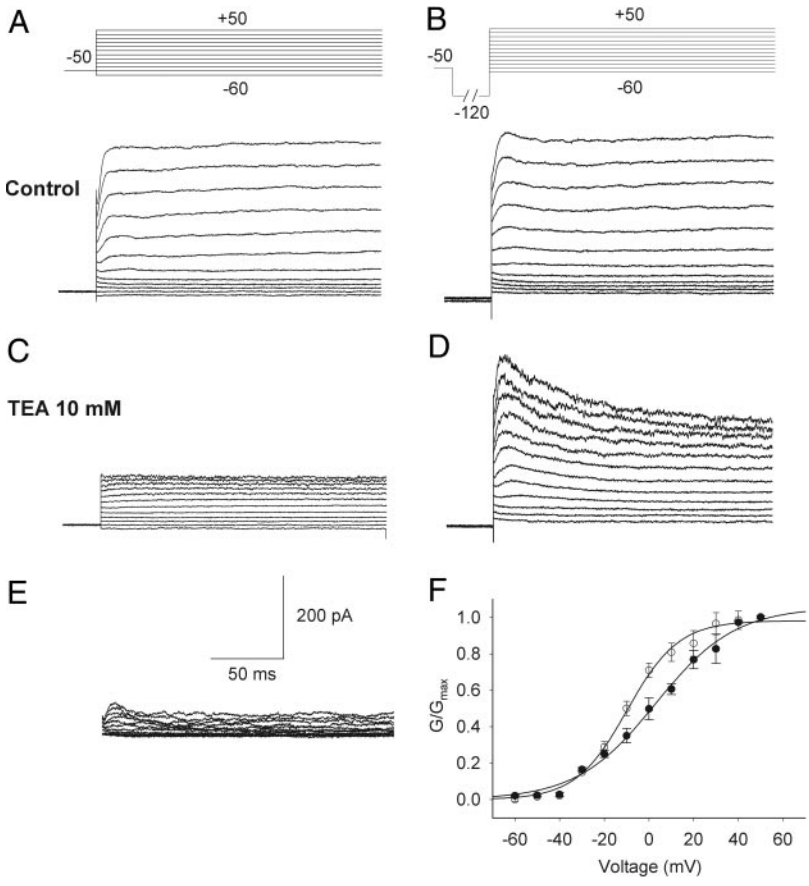

FIG. 1. Separation of 2 types of voltage-dependent K^+ currents in whole cell recordings. *A*: whole cell K^+ currents evoked by depolarizing voltage steps from a holding potential of −50 mV. The slow K^+ current (I_K) was activated by this voltage protocol. The voltage protocol is shown above the current traces. *B*: whole cell currents evoked by the same series of step depolarization except for a 600-ms conditioning step to −120 mV to activate the fast K^+ current (I_A). The −120-mV prepulse was truncated to facilitate the display of K^+ currents. The voltage protocol is shown above the current traces. *C*: when 10 mM TEA was applied to the bath solution, I_k currents reduced. The voltage protocol was the same as in *A*. *D*: when a −120-mV prepulse was used, 10 mM TEA in bath solution reduced I_K, emphasizing I_A. *E*: different currents were estimated by subtracting the records in *A* from those in *B*. The scale bars also apply to *A–D*. *F*: activation curves of the I_K isolated in A (○) and the I_A isolated in *E* (●). The conductance was determined from the maximal current amplitude divided by the K^+ ion driving force, which was calculated from the Nernst equation and normalized to the maximal conductance in a given series of voltages. The smooth lines are the fits to a Boltzmann function with 1 gate ($n = 4$). Error bars are ±SE. The current traces displayed at *A–D* were all recorded on the same cell.

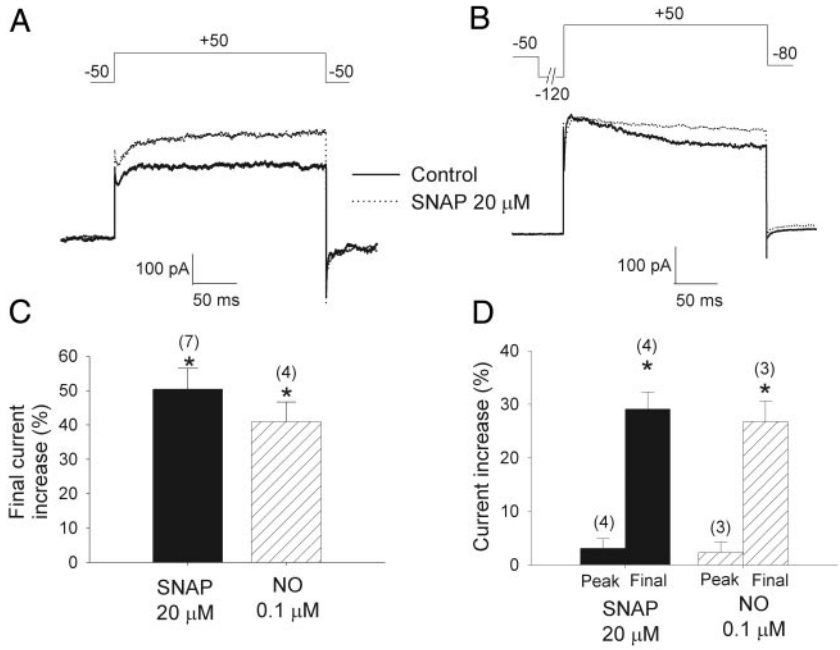

FIG. 2. Low concentrations of *S*-nitro-*N*-acetylpenicillamine (SNAP) and pure nitric oxide (NO) solution increase only the I_K currents but not I_A currents. *A* and *B*: whole cell K^+ currents before and after the application of 20 μM SNAP. The voltage protocols are displayed above the traces. The scale bars are shown under the current traces. I_K currents were increased after application of 20 μM SNAP in the bath solution. Averaged results are shown in *C*. When a 600-ms conditioning step to −120 mV was applied, 20 μM SNAP enhanced the final currents but the peak currents were left unchanged. Averaged results of the enhancement of peak and final currents for 20 μM SNAP are shown in *D*. The numbers of measurements are above each bar. *, significant difference between control and experimental group ($P < 0.05$).

cell I_K current (Fig. 2*A*). The effects of SNAP were very rapid, starting 30 s after the application of the reagent, and reaching maximal values in 5 min. At +50 mV, the current increased 50.4 ± 6.0% (Fig. 2*C*), which was significantly higher than the control neuron with no SNAP treatment. However, when a −120-mV conditioning pulse was applied, the peak current remained unchanged while the final currents increased (Fig. 2*B*). At +50 mV, the final currents increased 29.2 ± 2.3% compared with the control, whereas the peak current increased only 3.1 ± 1.8%, which was not significantly different from the control (Fig. 2*D*). This suggests that 20 μM SNAP had little effect on the I_A currents.

To exclude the possibility that SNAP stimulated the channel activity by a mechanism other than generation of NO, we examined the effect of pure NO solution directly micro-perfused onto the cell. Similar results were obtained when using pure NO solution. The I_K current significantly increased to 40.9 ± 5.8% at +50 mV when applied 0.1 μM pure NO solution to the cell (Fig. 2*C*). When a −120-mV conditioning pulse was applied, 0.1 μM NO only increased final current to 28.2 ± 3.8%, whereas the peak current was unchanged (2.3 ± 2.0% compared with that of control, $P > 0.05$; Fig. 2*D*). The effect of NO solution was faster than SNAP, starting 5 s after application and reached maximal values in 1 min.

High concentration of SNAP and pure NO decrease the whole cell K^+ current

When the concentration of SNAP was increased to 100 μM, a rapid reduction of whole cell K^+ current within 1 min was observed. The application of freshly prepared 100 μM SNAP to cells, held at −50 mV, resulted in fast reduction of the whole cell I_K current (Fig. 3*A*). At +50 mV, the current decreased 65.1 ± 1.2% (Fig. 3*C*), significantly lower than the control. When a −120-mV conditioning pulse was applied, both the peak current and the final currents decreased dramatically (Fig. 3*B*). At +50 mV, the final currents decreased 62.9 ± 5.6%, whereas the peak current decreased 59.8 ± 2.6% compared with the control ($P < 0.05$; Fig. 3*D*). This suggested that 100 μM SNAP decreased both I_K and I_A currents. The reductions of the current were irreversible and persisted after washing for 5 min.

A similar effect was detected when high concentrations of pure NO (0.5 μM) were used. At +50 mV, the averaged reduction was 62.5 ± 2.9% for I_K current when 0.5 μM NO was applied to the bath solution. The peak current and final current decreased 69.2 ± 6.6 and 65.8 ± 3.8%, respectively, when a −120-mV conditioning pulse was applied (Fig. 3*D*). The calibration of NO concentration released from SNAP is described in next section.

Calibration and quantitative measurement of NO release from SNAP

Because SNAP releases NO continuously, it is important to know the NO concentration in the bath solution for the electrophysiological experiments. A chemically modified NO sensor was used to calibrate the real-time NO oxidation current at successive steps after injection of 0.5 μM dissolved NO at each step to the bath solution. Figure 4*A* shows a typical calibration of the NO current-concentration curve obtained with a Nafion@Au working electrode at +800 mV (vs. Ag/AgCl) for the successive addition of 0.5 μM NO. With the addition of NO, the current generated from the oxidation of NO increased correspondingly. The *inset* shows that the correlation between the current response and the concentration of NO was linear, expressed as $I = 75.37 \times [NO] - 0.3143$ (correlation coefficient $r = 0.9998$, $P < 0.05$). Figure 4*B* illustrates an amperogram for the detection of NO released from SNAP with the same Nafion@Au working electrode at +800 mV (vs. Ag/AgCl). Each step corresponded to an addition of 20 μM of SNAP. The *inset* shows that the current response was linear to the square root of SNAP concentration, instead of SNAP concentration, expressed as $I = 2.135 \times [SNAP]^{1/2} - 0.1974$ ($r = 0.9990$, $P < 0.05$). The following equation summarizes the mathematical relation between the [NO] and the $[SNAP]^{1/2}$

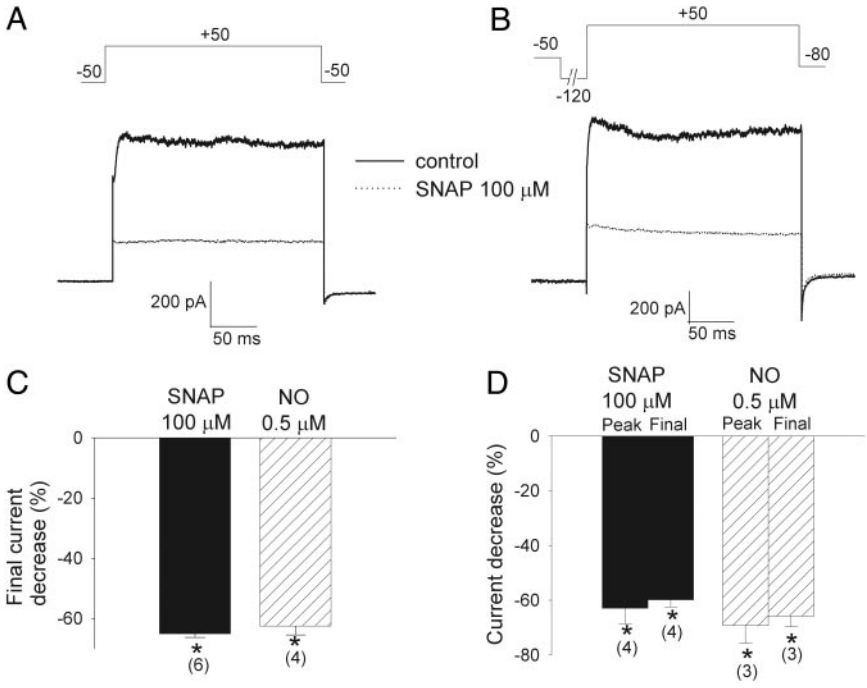

FIG. 3. High concentrations of SNAP and pure NO solution decrease both the I_K and I_A currents. *A* and *B*: whole cell K^+ currents before and after the application of 100 μM SNAP. The voltage protocols are displayed above the traces. The scale bars are shown under the current traces. I_K currents were decreased after the application of 100 μM SNAP in the bath solution. Averaged results are shown in *C*. Both peak and final currents were reduced when a 600-ms conditioning step to −120 mV was applied. Averaged results are shown in *D*. The numbers of measurements are above each bar. *, significant difference between control and experimental group ($P < 0.05$).

when both reagents produced an equal amount of current detected at the same electrode

$$[NO] = 0.0016 + 0.028 \times [SNAP]^{1/2} \quad (1)$$

Note that the current response (I) was expressed in nanoampere and the concentration of NO and SNAP was expressed in micromolar. These equations can be taken to calibrate the actual NO concentration released from the NO donor SNAP that was supplied to the relevant solution. Thus the calibrated NO concentration released by 20 and 100 μM SNAP were calculated to be 0.13 and 0.28 μM, respectively.

To ensure the NO levels measured in electrochemical experiments to be the same as the levels applied in the electrophysiological experiments, the calibration was done every time before starting the electrophysiological recording. A 5~10 mM stock solution of SNAP was made on the day of experiments and was stored at −20°C to minimize the degradation of SNAP.

Effect of SNAP and pure NO on K^+ single-channel activity

The whole cell voltage-clamp experiments described in the preceding text suggest that low concentration of SNAP (20 μM) and pure NO (0.1 μM) increased the I_K currents amplitude but not the I_A current. However, higher concentrations of SNAP (100 μM) and NO solution (0.5 μM) induced a blockade of both I_K and I_A K^+ currents. We further confirmed this effect of NO on single K^+ channel activity in cell-attached patches. The observation that I_K and I_A currents were differentially modified by different concentrations of NO suggests that NO may have kinetically distinct actions on the two major channels responsible for the K^+ current in this preparation. To clarify this issue, we focused on the I_K channel in the following single-channel recordings of this study.

The single-channel activities were recorded when a cell-attached patch was depolarized from 0 to 80 mV. The pipette

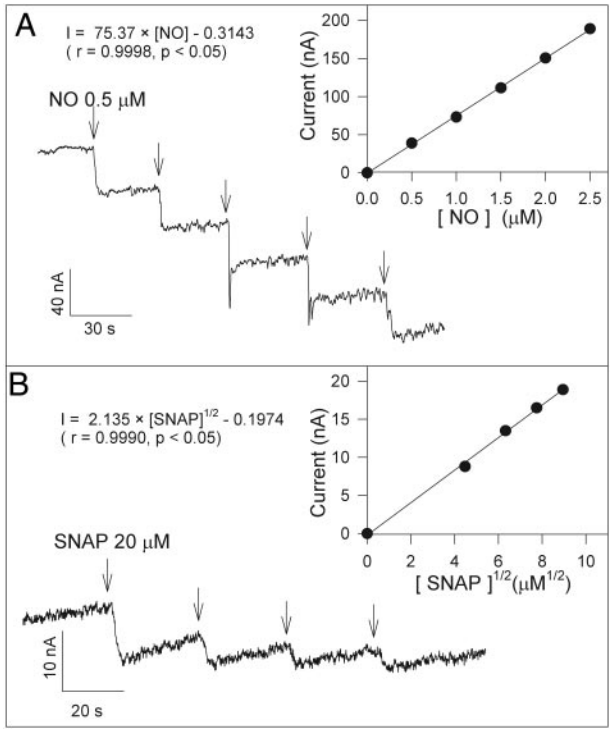

FIG. 4. An electrochemical calibration of SNAP for quantification of the released NO concentration. *A*: amperometric curves of NO detected by NO electrochemical sensor. ↓, each injection of 0.5 μM NO. *Inset*: dose-response curve for NO. The correlation between the current size and NO concentration is displayed above the traces. *B*: amperometric curves of different concentrations of SNAP. ↓, each injection of 20 μM SNAP. *Inset*: dose-response curve for SNAP. The correlation between the current size and SNAP concentration are shown above the traces. Au working vs. Ag/AgCl, E = 800 mV.

solution contained 140 mM KCl, similar to the expected intracellular [K^+], and thus the reversal potential for K^+ was close to 0 mV. Patch membrane potentials were calculated from the equation: V_{mem} = RMP $-V_{cmd}$, where V_{cmd} was the patch depolarization step, and RMP was the resting membrane potential. Figure 5, *A* and *B*, shows an analysis of the single-channel conductance. Currents recorded from one patch on depolarization to various voltages are shown in Fig. 5*A*. Figure 5*B* displays averaged single-channel current amplitude in four cells each. Currents were linearly related to membrane potentials, and the slope conductance corresponding to the regression line shown in figure was 45.8 pS at pipette [K^+] of 140 mM. The currents were sensitive to blockage of 10 mM TEA and 250 μM 4-aminopyridine (4-AP; Fig. 5, *C* and *D*). The ensemble averaged currents had a delayed rectifier property (Fig. 6*B*), suggesting that it was a single I_K channel.

Figure 6*A* illustrates the dual effect of SNAP on I_K channel activity. The addition of 40 μM SNAP significantly increased the channel NP_0 and the amplitude of the ensemble averaged current (Fig. 6*B*). In contrast to low concentration of SNAP, 100 μM SNAP decreased the channel activity and the amplitude of the ensemble averaged current. Figure 6*C* is a representative figure of the all-points amplitude histograms obtained under control condition and in the presence of 40 or 100 μM SNAP, showing that 40 μM SNAP increased NP_0 from 0.04 $\pm$ 0.01 to 0.49 $\pm$ 0.04 (n = 6) after adding SNAP into the bath solution, whereas 100 μM SNAP decreased NP_0 to 0.0002 $\pm$ 0.0003 (n = 8). Because a high dose of NO could trigger its effect by oxidizing thiol-containing protein, and several ion channels are reported to be redox-responsive (Al-Mustafa et al. 2001; Broillet et al. 1996; Xu et al. 1998), we determined whether the reducing agent dithiothreitol (DTT) could recover the channel activity. DTT has been widely used to investigate *S*-nitrosylation and redox mechanisms of various proteins, including I_k channel in guinea pig cardiomyocytes (Bai et al. 2004), Ca^{2+}-activated K^+ channels (Abderrahmane et al. 1998) and ryanodine receptors (Menshikova et al. 2000). DTT itself has no effect on the macroscopic whole cell and single-channel I_k currents (Fig. 7, *A* and *B*), consistent with the results from colonic smooth muscle (Prasad and Goyal 2004). Figure 6, *A* and *B*, shows that after adding 5 mM DTT into the bath solution containing 100 μM SNAP, the K^+ channel activities were restored and its NP_0 increased to 0.03 $\pm$ 0.01 (n = 6). Similarly, our whole cell results show that after treatment with 5 mM DTT, the current was recovered to ~65% of the control, which is comparable to single-channel data (Fig. 7C). The similarity in DTT effect (along with similar responses to 4-AP and TEA) on the whole cell currents and single-channel currents suggest that both currents arise from the activity of the same type of channel.

The summary of the results of dual effect of SNAP on K^+ channel NP_0 is shown in Fig. 8*A*, which demonstrates the variation of NP_0 with respect to changes in SNAP concentrations. It should be noted that the release of NO by SNAP is gradual and prolonged, being close to physiological conditions as demonstrated in the previous section when the NO sensor was used to measure the NO release from SNAP. Based on *Eq. 1*, 40 μM SNAP is equivalent to 0.18 μM of calibrated NO level and 100 μM SNAP is approaching to 0.30 μM of calibrated NO.

As stated before, to confirm whether the effect of SNAP on single-channel activity was due to generation of NO, we used pure NO solution to observe the NO effect on single channel activity. Figure 8*B* summarizes the results of experiments showing the effect of low concentration and high concentration of pure NO and 5 mM DTT on NP_0. A low concentration of NO (0.1 μM) increased the NP_0 from 0.04 $\pm$ 0.01 to 0.42 $\pm$ 0.10 (n = 5), whereas high concentrations of NO (0.5 μM) totally abolished the channel activity with NP_0 = 0.005 $\pm$

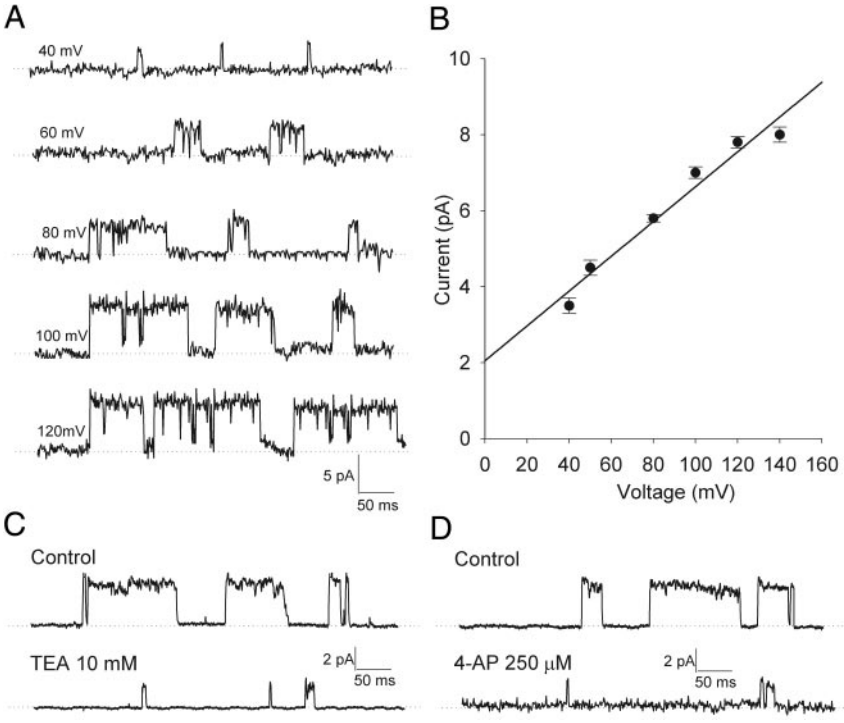

FIG. 5. Characterization of K^+ single channels. *A*: representative recordings obtained from 1 cell-attached patch on depolarization from 0 mV to the voltages indicated with pipette [K^+] 140 mM. · · · , closed-channel current. *B*: single-channel current-voltage relationship. The slope conductance from a linear regression between 40 and 140 mV is 45.8 pS. *C*: recordings from same patch before and after 10 mM TEA was applied. *D*: recordings from same patch in the absence and presence of 250 μM 4-aminopyridine (4-AP). The patch was depolarized from 0 to 80 mV in *C* and *D*.

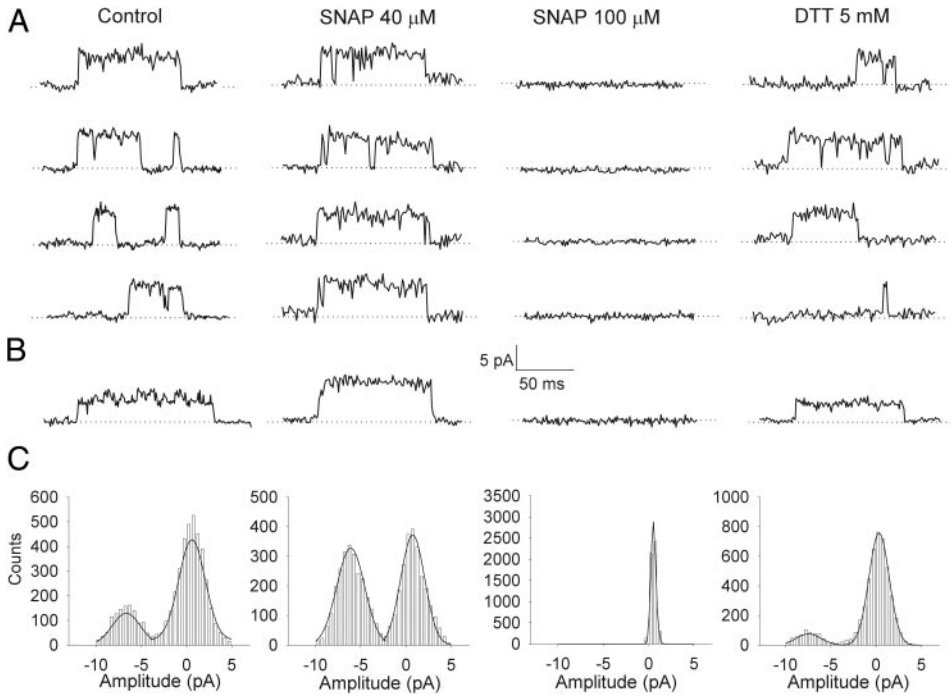

FIG. 6. Different concentrations of SNAP exerted differential effects on K^+ single-channel activities in cell-attached recordings. *A*: representative single-channel sweeps before (control) and during bath application of 40 μM, 100 μM SNAP, and 5 mM dithiothreitol (DTT). In all traces, the patch was depolarized from 0 to 80 mV. The scale bar is applied to all the traces. Closed channel current is indicated by dotted line. *B*: ensemble averaged current from 60 consecutive sweeps recorded in the control condition, 40 μM, 100 μM SNAP, and 5 mM DTT. *C*: all-points amplitude histograms of channel currents were obtained under control condition, in the presence of 40 μM SNAP, 100 μM SNAP, and 5 mM DTT.

0.0005 ($n = 6$). The channel activities could be recovered by adding 5 mM DTT, with NP_0 increased to 0.03 ± 0.01 ($n = 5$).

Effect of PKG and cGMP inhibitor on K^+ channel

Many of the cellular effects of NO are mediated by soluble guaylate cyclase (sGC) and cGMP. It has been shown that increases in cGMP levels mediate a large number of physiological actions of NO. Either nitregic nerve stimulation or administration of NO donors increases intracellular cGMP concentrations (Bredt and Snyder 1989; Torphy et al. 1986). To further explore cGMP signaling in the facilitation of I_K channel activity, we used the inhibitors for sGC and cGMP dependent protein kinase G (PKG) to inhibit their actions. Figure 9C shows that under 40 μM SNAP treatment, the averaged NP_0 is 0.48 ± 0.15 ($n = 6$). However, in the presence of 10 μM 1H-[1,2,4]oxadiazolo[4,3-a]quinoxalin-1-one (ODQ), a highly selective inhibitor of sGC, the averaged NP_0 values in the presence of 40 μM SNAP were significantly decreased to 0.02 ± 0.01 ($n = 3$; Fig. 9, *A* and *C*). The reduction of channel activity could be reversed by addition of a membrane-permeable cGMP analogue, 8-Br-cGMP. Moreover, 100 μM 8-Br-cGMP has similar effect as 40 μM SNAP, it significantly increased NP_0 from 0.04 ± 0.02 to 0.38 ± 0.14 (Fig. 9, *B* and *C*). Another sGC inhibitor, methylene blue (MB) 300 μM (C. H. Chen et al. 1998; Kang et al. 2005; Pineda et al. 1996) also significantly reduced NP_0 in the presence of 40 μM SNAP to 0.19 ± 0.06 ($n = 5$; Fig. 9*C*). These results indicate that NO stimulates sGC and elevates intracellular cGMP, which leads to channel activation.

In the next step, we examined whether the cGMP-dependent action of NO was indeed involved through a PKG-dependent signaling transduction pathway. As shown in Fig. 9*C*, H-8, a specific inhibitor of PKG (Bolotina et al. 1994; C. H. Chen et al. 1998; Pineda et al. 1996), inhibited the enhanced channel activity by 40 μM SNAP. The averaged value of NP_0 in the presence of 40 μM SNAP was reduced to 0.11 ± 0.02 ($n = 6$). That the effect of H-8 was induced by inhibiting PKG was further confirmed by using Rp-8-Br-PET-cGMP, a more specific inhibitor of PKG than H-8. Figure 9*C* shows that addition of 100 μM Rp-8-Br-PET-cGMP completely abolished the effect of 40 μM SNAP. In addition, in the presence of 100 μM Rp-8-Br-PET-cGMP, the cGMP analogue 8-Br-cGMP 100 μM failed to reactivate the channel, suggesting that PKG-

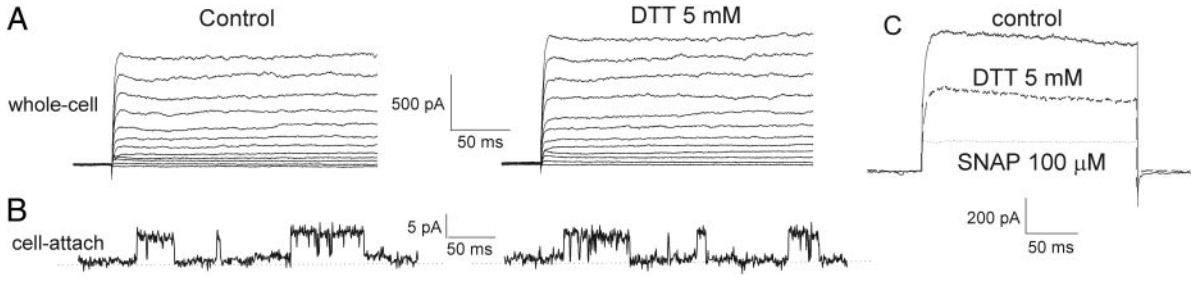

FIG. 7. Effect of 5 mM DTT on either whole cell or cell-attached I_K currents. *A*: whole cell I_K currents before and after application of 5 mM DTT in the bath solution. The currents were evoked by depolarizing voltage steps from −60 to 50 mV with holding potential of −50 mV. The currents traces were recorded from the same cell. *B*: cell-attached recordings in the absence and presence of 5 mM DTT on the same cell. The cell was depolarized from 0 to +80 mV. ···, closed channel. *C*: addition of 100 μM SNAP dramatically reduced the whole cell I_K currents, which can be recovered by 5 mM DTT.

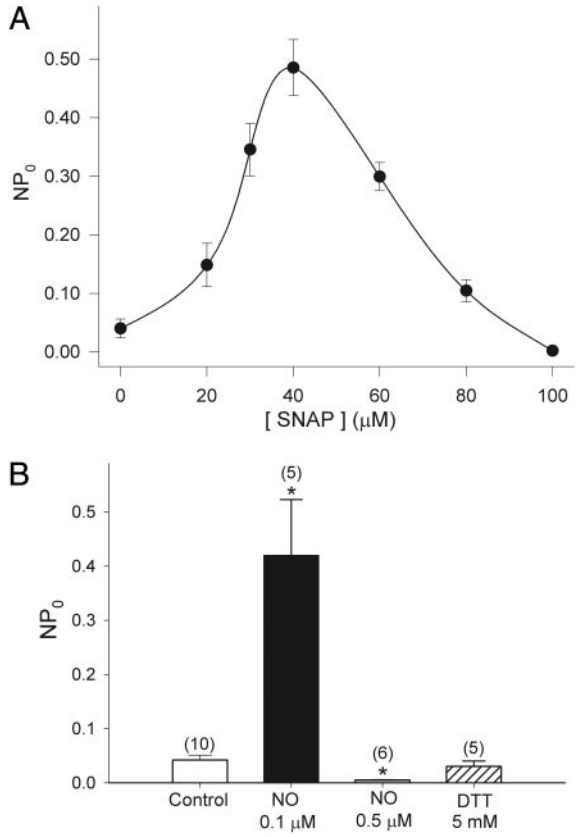

FIG. 8. Dose-dependent effect of SNAP and pure NO on the open probability of K^+ single channel. *A*: dose-response curve of SNAP on the single-channel NP_0. Data were obtained from 6 experiments. *B*: summary of the effect of 0.1 μM NO, 0.5 μM NO, and 5 mM DTT on single-channel NP_0. The numbers of measurements are above each bar. *Significant difference between control and experimental group ($P < 0.05$).

dependent signal transduction pathway was involved in the facilitation of K^+ channel by a low dose of SNAP ($\leq$40 μM) or pure NO (0.1 μM).

Effect of superoxide on K^+ channel activity

After establishing the optimum concentration of SNAP that could maximally increase the channel open probability, we investigated whether superoxide anion was involved in the process of the SNAP regulation of K^+ channel. Several lines of evidence suggested that superoxide itself may affect K^+ channel activity directly or through oxidizing K^+ channel associated proteins (Armstead 2001; Brzezinska et al. 2005; Van der Vlies et al. 2002). The results in Figs. 6–8 show that reducing agent DTT was able to recover the channel open probability from a high dose of SNAP or NO solution, indicating that regulation process by high levels of NO maybe due to an oxidation mechanism. To test this hypothesis, we then test whether superoxide itself affects channel activity by applying a superoxide-generating agent, KO_2, into the bath solution. KO_2 spontaneously releases $O_2^{\bullet -}$ in the solution phase. Figure 10A illustrates an inhibitory effect of superoxide on the channel activity. The channel openings were recorded 3 min after adding KO_2. Figure 10*A* shows that 20 μM KO_2 dramatically decreased the NP_0 from 0.04 $\pm$ 0.01 to 0.009 $\pm$ 0.0004 (n = 8). When the concentration of KO_2 was further increased to 40 μM, the channel openings were entirely abolished. The open probability decreased as a function of the concentration of KO_2 increased from 0 to 40 μM. The reduction of channel activity could be reversed by 800 Unit of superoxide dismutase (SOD; Fig. 10*A*).

The ability of DTT to reverse the effect of KO_2 was also examined. The exposure to 5 mM DTT for 2–3 min restored channel activity (Fig. 10*A*), suggesting a redox-dependent regulation of the K^+ channel activity by superoxide.

However, when we added 800 U of superoxide dismutase (SOD) to the typical control sample and observed the channel activity, there was no significant difference of NP_0 values between the control and the SOD-treated group (Fig. 10*B*). When 800 U of SOD and 40 μM SNAP were co-introduced, a significant increase in the NP_0 (0.4232 $\pm$ 0.1173) was observed (Fig. 10*B*). When 100 μM SNAP was added with 800 U of SOD, the channels almost closed (NP_0 = 0.003 $\pm$ 0.003; Fig. 10*B*). Interestingly, when the reducing agent DTT was applied to the silent channel in the presence of high-dose SNAP, we found recovering of NP_0 of the channel (NP_0 = 0.028 $\pm$ 0.012; Fig. 10*B*). A comparison of the data in Fig. 10*B* with those in the absence of SOD (Fig. 8*A*) showed that there was no significant difference in the effect of SNAP with or without SOD on K^+ channel. These results suggested that superoxide anion ($O_2^{\bullet -}$) did not exert any detectable effect on the SNAP regulation of K^+ channel under our experimental conditions.

DISCUSSION

Our results have shown that NO has a dual effect on regulating the I_K channel, which is a major component of K^+ currents in cultured mouse cerebral neocortical neurons. First low concentrations of NO increased the whole cell I_K currents. NO also increased single I_K channel activity by increasing the NP_0, as measured in the cell-attached patch recordings. Second, high concentrations of NO inhibited the whole cell I_K currents and single I_K channel activity by decreasing the NP_0, the total open probability of channel. The cGMP signaling pathway is involved in the facilitation of I_K channel by low NO concentration. The reduction of I_K currents by high NO concentration can be reversed by DTT, suggesting a redox-mechanism involved in this signaling pathway.

Mode of NO action in modulating K^+ channel can be specific to the channel type and differentially corresponding to NO concentration

Since the discovery of NO as a modulator of neuronal function in the brain (Garthwaite et al. 1988), many studies have shown that the role of NO in CNS is highly diverse. For example, NO inhibits outwardly rectifying K^+ current in both the whole cell and the cell-attached patches in type I hair cells from rat semicircular canals (Chen and Eatock 2000). However, Browning et al. (1998) found that in cultured sympathetic ganglionic neurons, NO exerts dual opposing effects on neuronal potassium conductances, namely an inward current shift mediated through an inhibition of calcium-dependent potassium currents and induction of an outward current mediated by activation of the potassium delayed rectifier channel. The controversial effect of NO on K^+ channel may be due to the

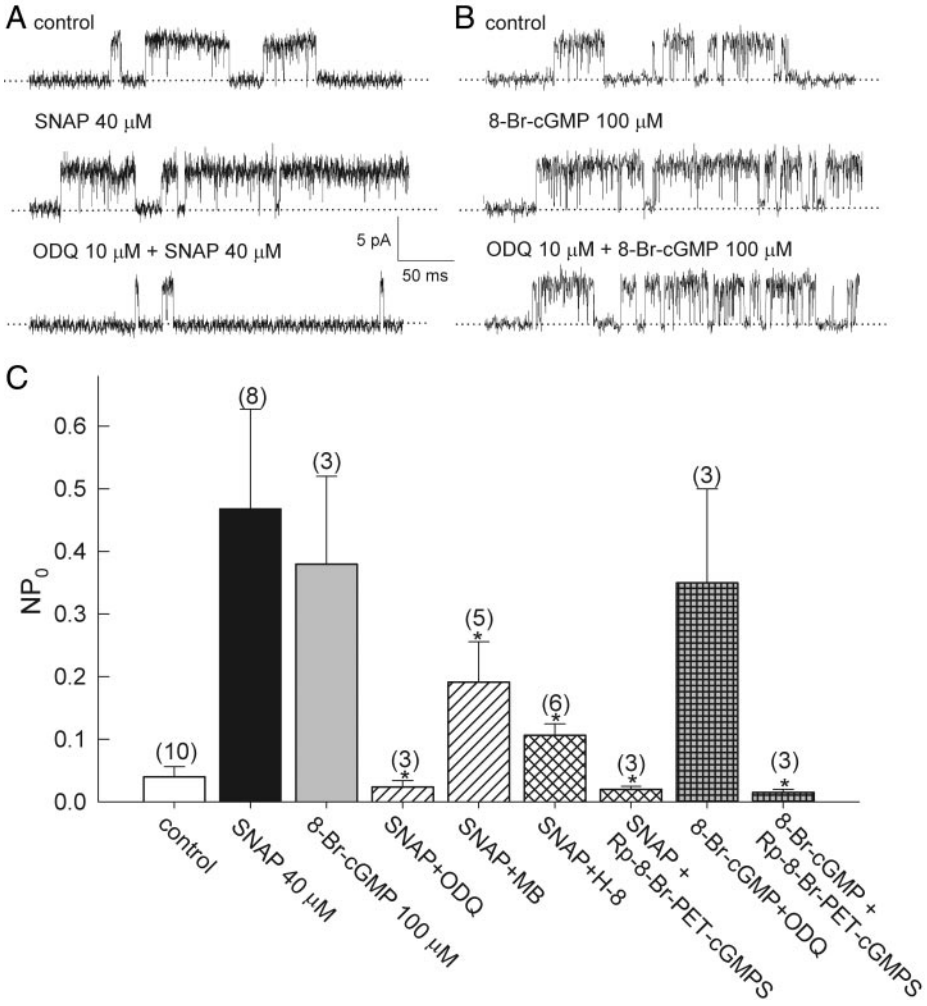

FIG. 9. The role of cGMP and cGMP-dependent protein kinase G (PKG) involved in the effect of SNAP on K^+ single-channel activities. *A*: representative single-channel sweeps before (control) and during bath application of 40 μM SNAP in the absence and in the presence of 10 μM ODQ. *B*: representative single-channel sweeps before and during bath application of 100 μM 8-Br-cGMP in the absence and in the presence of 10 μM ODQ. In all traces, the patch was depolarized from 0 to 80 mV. The scale bar is applied to all the traces. · · · , closed channel current. *C*: summary of the actions of 10 μM 1H-[1,2,4]oxadiazolo[4,3-a]quinoxalin-1-one (ODQ), 300 μM methylene blue (MB; sGC inhibitors), and 1 μM *N*-[2-(methylamino)ethyl]-5-isoquinolinesulfonamide (H-8), 100 μM Rp-8-Br-PET-cGMPS (PKG inhibitors) on augmentation of K^+ single-channel NP_0 by 40 μM SNAP or 100 μM 8-Br-cGMP (cell-membrane-permeable cGMP analog). Numbers of experiments are indicated above each bar. *, significant difference in comparison to the value at SNAP 40 μM ($P < 0.05$).

different brain regions by which NO acts on or that the exact effective concentrations of NO at any particular instant are varied. Therefore we proceed to measure such concentrations using electrochemical NO sensor in this investigation. Based on *Eq. 1*, 20 μM SNAP equivalent to 0.13 μM of calibrated NO would lead to an increase in K^+ channels opening. In contrast, 100 μM SNAP equivalent to 0.30 μM of calibrated NO would tend to close these channels. In recent years, the relationship between NO concentrations and its cellular physiology has caught sufficient attention. Development of sensitive and selective analytical methods for the measurement of NO in biological systems has received great interest. NO is difficult to measure in vivo because of its short half-life. In addition, the diffusion rates of NO in different tissues, redox environment and compartmentalization of NO targets are important factors in determining NO actions. Concentrations of NO in different tissues can vary from a few nanomolar to micromolar. In rat cerebellar slices, endogenous NO production ranges from 8 to 58 nM (Shibuki 1990). On stimulation of NMDA receptor, NO concentration increased from a low nanomolar range up to ~200 nM in rat hippocampal slices (Ledo et al. 2002). In peripheral macrophages and endothelial cells, concentrations of NO could reach up to ~1 μM (B. Chen et al. 1998; Malinski et al. 1993).

The modulation of I_k channels by NO has been investigated in vascular smooth muscle (Li et al. 1997; Waldron and Cole 1999). It showed that the open probability of a 49.1 pS I_k channel increased 10- to 25-fold by NO donor NONOate in a concentration-dependent manner (Li et al. 1997). The I_k channels in our study showed a conductance of 45.8 pS, in agreement with those reported elsewhere, such as those of bovine arterial smooth muscle (49.1 pS) (Li et al. 1997), rabbit portal vein smooth muscle (42 pS) (Ogata et al. 1997), canine atrial myocytes (35.5 pS) (Yue et al. 1996), and rat dorsal ganglion neurons (55 pS) (Safronov et al. 1996).

Voltage-dependent K^+ channel is widely distributed throughout the brain. It is known that changes in functions of K^+ channels will directly affect the neuronal activity because K^+ channels function to set a cell's resting potential, repolarize the cell after an action potential, and control the shape and the threshold of action potential (Nestler et al. 2001). Therefore the modification of neuronal K^+ currents by NO may affect neuronal membrane potential and thereby cause changes in the neuronal activity. Several lines of evidence have shown that delayed-rectifier K^+ channels were involved in the pathological process of neuronal death mediated by NO (Bossy-Wetzel et al. 2004; Yu et al. 1997, 1998). The transient, A-type K^+ channel was proposed to correlate with the induction of long-term potentiation (Johnston et al. 2003). The voltage-dependent K^+ channels are expressed in both pre- and postsynaptic areas although the distribution patterns in cell body, dendrite, axon and axon terminal are different. As a possible retrograde

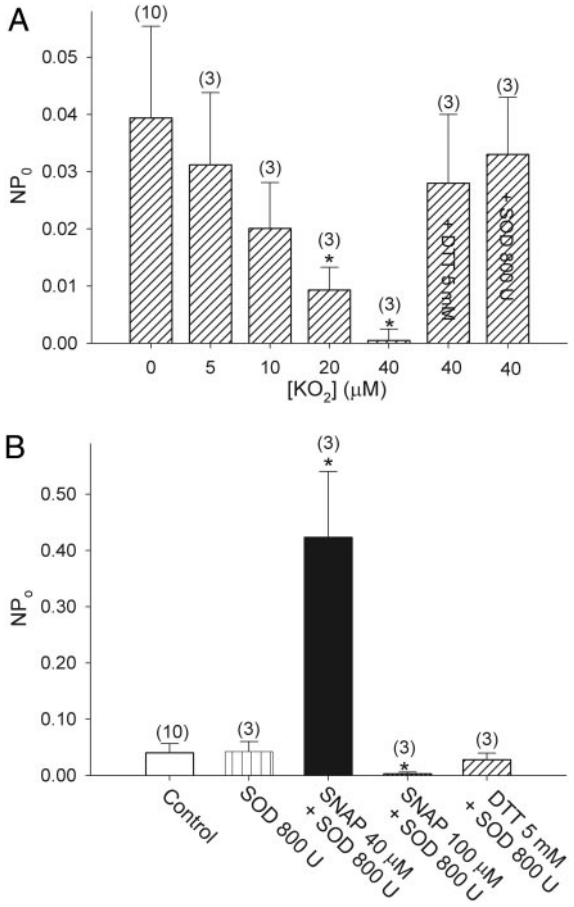

FIG. 10. Effect of superoxide agents on regulation of single K^+ channel activities. *A*: summary of dose-response curve of KO_2 on single-channel NP_0. The channel activity recovered after the addition of 5 mM DTT and 800 U superoxide dismutase (SOD). Numbers of experiments are indicated above each bar. *, significant difference in comparison to the control ($P < 0.05$). B: summary of the action of 800 U SOD on the augmentation of K^+ + single-channel $NP_0$0 by 40 μM SNAP. There was no significant difference between the NP_0 value in the presence of 800 U SOD and the control ($P > 0.05$). No significant difference was observed between the values in the absence and in the presence of 800 U SOD ($P > 0.05$).

messenger, NO can regulate both pre- and postsynaptic K^+ channels, hence modulate neuronal synaptic plasticity.

Involvement of cGMP in NO signaling pathway

It is well known that NO donors activate the guanylate cyclase and cGMP-dependent pathways in most cells (Fischmeister and Mery 1996; White 1999). There is ample evidence showing NO-cGMP signaling cascade in the CNS and peripheral tissues. In fact, we are probably the first to demonstrate that a cGMP-dependent pathway in cerebral cortical neurons could be involved in facilitating the effect of low NO levels on the I_K channel. The application of sGC inhibitors, ODQ and MB, and specific PKG inhibitors, H-8 and Rp-8-Br-PET-cGMP, abolished the facilitating effect of low NO concentration on I_K channel. The addition of a cell-membrane-permeable cGMP analogue, 8-Br-cGMP, reversed the inhibitory effect of ODQ but not the effect of PKG inhibitor Rp-8-Br-PET-cGMP. Thus it can be concluded that low NO levels stimulated channel activity through the activation of sGC, leading to subsequent elevation of intracellular cGMP and activation of the PKG-mediated signaling pathway. Our results are consistent with findings in apical K^+ channel of rat kidney, ATP-sensitive K^+ channel from ventricular cells of guinea-pig hearts, and Ca^{2+}-activated K^+ channel in posterior pituitary nerve terminal (Klyachko et al. 2001; Lu and Wang 1996; Lu et al. 1998; Shinbo and Iijima 1997). Lu et al. (1998) found that NO enhanced K^+ channel activity in cell-attached patches and the enhancement was abolished by ODQ.

Moreover, the intracellular concentration of cGMP dramatically increased after SNAP application. It was reported that intracellular cGMP concentrations increased $\leq$10 folds 2–3 min just after administration of NO donors (Bredt and Snyder 1989; Lu et al. 1998). We observed that the facilitating effect of low concentrations of NO or SNAP was very fast, starting in $<$5 s of pure NO application. We used whole cell and cell-attached configurations in our study because these two configurations maintained cells in their physiological environment. Although we did not include ATP and GTP in out patch pipette solution in whole cell experiments, the fast effect of low concentrations of SNAP or NO is unlikely due to *S*-nitrosylation mechanisms (i.e., the process of transferring a NO-group to a protein) because the half-reaction time of *S*-nitrosylation is much longer (Ahern et al. 2002). However, we cannot exclude the possibility that other cGMP-independent pathway may also involve in the facilitating effect of low level NO on I_K channels.

Redox mechanism induced by NO

In recent years, discovery of endogenous sources of oxidizing and reducing agents have prompted the recognition of redox modulation of protein function and direct effect of NO on *S*-nitrosylation as an important mechanism for many cell types, thus affecting a variety of proteins (Jaffrey et al. 2001; Stamler et al. 1992, 2001). A regulatory mechanism of ion channel activity involving sulfhydryl to disulfide conversion has been described previously and "regulatory thiols" have been demonstrated to be related to activities of K^+ channel (George and Shibata 1995; Trapp et al. 1998), *N*-methyl-D-aspartate-receptor channels (Choi et al. 2000), P2X receptors (Ennion and Evans 2002), and ryanodine receptor calcium release channels (Xia et al. 2000).

Being a reactive-free radical, the chemical reactions of NO are largely dictated by its redox state. Increasing evidence suggests that the various redox states of NO exist endogenously in biological tissues. It is established that NO can react with thiol-containing biomolecules (RSH) such as cysteine and glutathione (GSH) to form *S*-nitrosothiols (RSNOs), which then release nitrogen-containing compounds, including NO (Miao et al. 2000; Moran et al. 2001; Sheu et al. 2000). Further oxidation of critical thiols can possibly form disulfide bonds. This implies that high concentrations of NO derived from a high dose of SNAP (100 μM) or the NO solution (0.5 μM) could modify K^+ channel by oxidation. We have found that decreases in channel activity elicited by NO could not be readily reversed by simply washing with perfusing solution. If this seemingly irreversible property was a consequence of NO oxidation or formation of adducts with free SH groups, such as cysteine residues on the K^+ channel protein (or a closely associated regulatory protein), leading to disulfide-bound formation, it should be possible to reverse this effect with a

reducing agent (sulfhydryl-regenerating agent) such as DTT (Miao et al. 2000). The data presented earlier in Figs. 6–8 showed that 5 mM DTT was able to recover the channel open probability from a high dose of SNAP or NO solution. Moreover, a similar effect of DTT was observed for the superoxide producing agent KO_2 (Fig. 10). These data suggests that part of NO regulation process, particularly when the concentration of NO reached a critically high level, was due to an oxidation mechanism and could be reversed by reducing agents.

Our preliminary results showed that superoxide radical inhibits the activity of the I_K channel. It is known that in the absence of the NOS substrate, arginine, NOS does not generate any NO (Pou et al. 1992). It is further noted that at low concentrations of arginine, a new catalytic function of NOS is to generate superoxide radicals (Xia et al. 1996). Because the reaction of superoxide dismutase with superoxide anion is less efficient than the combination of superoxide with trace levels of NO to form peroxynitrite (Beckman and Koppenol 1996). The inhibition of K^+ channels by superoxide may explain the toxicity of superoxide related to NO and NOS in the CNS. However, the effect of NO in the presence of superoxide on the K^+ channels is largely unknown and awaits further investigation.

In summary, the present study demonstrates observation of a dual effect of NO on I_K channel in mouse neocortical neurons. Both the NO-cGMP signaling and the NO-triggered redox mechanism are involved in the modulation of I_K channel activity. These findings have a fundamental relevance to neuronal synaptic activity because K^+ channels play an important role in controlling the overall neuron excitability.

ACKNOWLEDGMENTS

We thank Dr. David Lovinger at National Institute on Alcohol Abuse and Alcoholism and Dr. Wendy Fung at Neuroscience Research Institute of Peking University for a critical reading and useful discussion of this work.

GRANTS

The work was partially supported by Academic Research Grants R-154-000-113-112 and R-154-000-228-112, National University of Singapore, to F.-S. Sheu. N.-L.R. Han is a Singapore Millennium Foundation Postdoctoral Fellow.

REFERENCES

Abderrahmane A, Salvail D, Dumoulin M, Garon J, Cadieux A, and Rousseau E. Direct activation of K(Ca) channel in airway smooth muscle by nitric oxide: involvement of a nitrothiosylation mechanism? *Am J Respir Cell Mol Biol* 19: 485–497, 1998.

Ahern GP, Klyachko VA, and Jackson MB. cGMP and S-nitrosylation: two routes for modulation of neuronal excitability by NO. *Trends Neurosci* 25: 510–517, 2002.

Al-Mustafa AH, Sies H, and Stahl W. Sulfur-to-nitrogen transnitrosation: transfer of nitric oxide from S-nitroso compounds to diethanolamine and the role of intermediate sulfur-to-sulfur transnitrosation. *Toxicology* 163: 127–136, 2001.

Armstead WM. Vasopressin-induced protein kinase C-dependent superoxide generation contributes to ATP-sensitive potassium channel but not calcium-sensitive potassium channel function impairment after brain injury. *Stroke* 32: 1408–1414, 2001.

Baughman RW, Huettner JE, Jones KA, and Khan AA. Cell culture of neocortex and basal forebrain from postnatal rats. In: *Culturing Nerve Cells,* edited by Banker G and Goslin. K. Cambridge, MA: MIT Press, 1991, p. 227–249.

Bai CX, Takahashi K, Masumiya H, Sawanobori T, and Furukawa T. Nitric oxide-dependent modulation of the delayed rectifier K^+ current and the L-type Ca^{2+} current by ginsenoside Re, an ingredient of Panax ginseng, in guinea-pig cardiomyocytes. *Br J Pharmacol* 142: 567–575, 2004.

Beckman JS and Koppenol WH. Nitric oxide, superoxide, and peroxynitrite: the good, the bad, and ugly. *Am J Physiol Cell Physiol* 271: C1424–1437, 1996.

Bedioui F, Trevin S, and Devynck J. The use of gold electrodes in the electrochemical detection of nitric oxide in aqueous solution. *J Electroanal Chem* 377: 295–298, 1994.

Bolotina VM, Najibi S, Palacino JJ, Pagano PJ, and Cohen RA. Nitric oxide directly activates calcium dependent potassium channels in vascular smooth muscle. *Nature* 368: 850–853, 1994.

Bossy-Wetzel E, Talantova MV, Lee WD, Scholzke MN, Harrop A, Mathews E, Gotz T, Han J, Ellisman MH, Perkins GA, and Lipton SA. Crosstalk between nitric oxide and zinc pathways to neuronal cell death involving mitochondrial dysfunction and p38-activated K^+ channels. *Neuron* 41: 351–365, 2004.

Bredt DS, Hwang PM, and Snyder SH. Localization of nitric oxide synthase indicating a neural role for nitric oxide. *Nature* 347: 768–770, 1990.

Bredt DS and Snyder SH. Nitric oxide mediates glutamate-linked enhancement of cGMP levels in the cerebellum. *Proc Natl Acad Sci USA* 86: 9030–9033, 1989.

Bredt DS and Snyder SH. Transient nitric oxide synthase neurons in embryonic cerebral cortical plate, sensory ganglia, and olfactory epithelium. *Neuron* 13: 301–313, 1994.

Broillet MC and Firestein S. Direct activation of the olfactory cyclic nucleotide-gated channel through modification of sulfhydryl groups by NO compounds. *Neuron* 16: 377–385, 1996.

Browning KN, Zheng ZL, Kreulen DL, and Travagli RA. Effects of nitric oxide in cultured prevertebral sympathetic ganglion neurons. *J Pharmacol Exp Ther* 286: 1086–1093, 1998.

Brzezinska AK, Lohr N, and Chilian WM. Electrophysiological effects of O2*- on the plasma membrane in vascular endothelial cells. *Am J Physiol Heart Circ Physiol* 289: H2379–2386, 2005.

Chen B, Keshive M, and Deen WM. Diffusion and reaction of nitric oxide in suspension cell cultures. *Biophys J* 75: 745–754, 1998.

Chen CH, Houchi H, Ohnaka M, Sakamoto S, Niwa Y, and Nakaya Y. Nitric oxide activates Ca^{2+}-activated K^+ channels in cultured bovine adrenal chromaffin cells. *Neurosci Lett* 248: 127–129, 1998.

Chen JW and Eatock RA. Major potassium conductance in type I hair cells from rat semicircular canals: characterization and modulation by nitric oxide. *J Neurophysiol* 84: 139–151, 2000.

Choi YB, Tenneti L, Le DA, Ortiz J, Bai G, Chen HS, and Lipton SA. Molecular basis of NMDA receptor-coupled ion channel modulation by S-nitrosylation. *Nat Neurosci* 3: 15–21, 2000.

Do JS and Wu KJ. Anodic oxidation of nitric oxide on Au/Nafion: kinextics and mass transfer. *J App Electrochem* 31: 437–443, 2001.

Ennion SJ and Evans RJ. Conserved cysteine residues in the extracellular loop of the human P2X(1) receptor form disulfide bonds and are involved in receptor trafficking to the cell surface. *Mol Pharmacol* 61: 303–311, 2002.

Fischmeister R and Mery PF. Regulation of cardiac calcium channels by cGMP and NO. In: *Molecular Physiology and Pharmacology of Cardiac Ion Channels and Transporters,* edited by Morad M, Ebashi S, Trautwein W, and Kurachi Y. Dordrecht, Netherlands: Kluwer Academic, 1996, p. 93–105.

Garthwaite J, Charles SL, and Chess-Williams R. Endothelium-derived relaxing factor release on activation of NMDA receptors suggests role as intercellular messenger in the brain. *Nature* 336: 385–388, 1988.

George MJ and Shibata EF. Regulation of calcium-activated potassium channels by *S*-nitrosothiol compounds and cyclic guanosine monophosphate in rabbit coronary artery myocytes. *J Investig Med* 43: 451–458, 1995.

Goslin K and Banker G. Rat hippocampal neurons neurons in low-density culture. In: *Culturing Nerve Cells,* edited by Banker G and Goslin K. Cambridge, MA: MIT Press, 1991, p. 251–281.

Hamill OP, Huguenard JR, and Prince DA. Patch-clamp studies of voltage-gated currents in identified neurons of the rat cerebral cortex. *Cereb Cortex* 1: 48–61, 1991.

Hille B. *Ion Channels of Excitable Membranes.* Sunderland, MA: Sinauer, 1992.

Jaffrey SR, Erdjument-Bromage H, Ferris CD, Tempst P, and Snyder SH. Protein *S*-nitrosylation: a physiological signal for neuronal nitric oxide. *Nat Cell Biol* 3: 193–197, 2001.

Johnston D, Christie BR, Frick A, Gray R, Hoffman DA, Schexnayder LK, Watanabe S, and Yuan LL. Active dendrites, potassium channels and synaptic plasticity. *Phil Trans R Soc Lond B Biol Sci* 358: 667–674, 2003.

Kang YJ, Sohn JT, and Chang KC. Relaxation of canine corporal smooth muscle relaxation by ginsenoside saponin Rg3 is independent from eNOS activation. *Life Sci* 77: 74–84, 2005.

Klyachko VA, Ahern GP, and Jackson MB. cGMP-mediated facilitation in nerve terminals by enhancement of the spike afterhyperpolarization. *Neuron* 31: 1015–1025, 2001.

Ko GY and Kelly PT. Nitric oxide acts as a postsynaptic signaling molecule in calcium/calmodulin-induced synaptic potentiation in hippocampal CA1 pyramidal neurons. *J Neurosci* 19: 6784–6794, 1999.

Lang RJ and Watson MJ. Effects of nitric oxide donors, *S*-nitroso-L-cysteine and sodium nitroprusside, on the whole-cell and single channel currents in single myocytes of the guinea-pig proximal colon. *Br J Pharmacol* 123: 505–517, 1998.

Lantoine F, TS, Bedioui F, and Devynck J. Selective and sensitive electrochemical measurement of nitric oxide in aqueous solution - discussion and new results. *J Electroanal Chem* 392: 85–89, 1995.

Ledo A, Barbosa RM, Frade J, and Laranjinha J. Nitric oxide monitoring in hippocampal brain slices using electrochemical methods. *Methods Enzymol* 359: 111–25, 2002.

Levitan I. Modulation of ion channels in neurons and other cells. *Annual Rev Neurosci* 11: 119–136, 1988.

Li PL, Zou AP, and Campbell WB. Regulation of potassium channels in coronary arterial smooth muscle by endothelium-derived vasodilators. *Hypertension* 29: 262–267, 1997.

Lu M and Wang WH. Nitric oxide regulates the low-conductance K channel in the basolateral membrane of the collecting duct of the rat kidney. *Am J Physiol Cell Physiol* 270: C1336–C1342, 1996.

Lu M, Wang X, and Wang WH. Nitric oxide increases the activity of the apical 70-pS K^+ channel in TAL of rat kidney. *Am J Physiol Renal Physiol* 274: F946–F950, 1998.

Malinski T, Taha Z, Grunfeld S, Patton S, Kapturczak M, and Tomboulian P. Diffusion of nitric oxide in the aorta wall monitored in situ by porphyrinic microsensors. *Biochem Biophys Res Commun* 193: 1076–1082, 1993.

Menshikova EV, Cheong E, and Salama G. Low *N*-ethylmaleimide concentrations activate ryanodine receptors by a reversible interaction, not an alkylation of critical thiols. *J Biol Chem* 275: 36775–36780, 2000.

Miao HH, Ye JS, Wong SL, Wang BX, Li XY, and Sheu FS. Oxidative modification of neurogranin by nitric oxide: an amperometric study. *Bioelectrochemistry* 51: 163–173, 2000.

Moran LK, Gutteridge JM, and Quinlan GJ. Thiols in cellular redox signalling and control. *Curr Med Chem* 8: 763–772, 2001.

Nestler EJ, Hyman SE, and Malenka RC. *Molecular Neuropharmacology: A Foundation for Clinical Neuroscience.* New York; McGraw-Hill, 2001.

Ogata R, Kitamura K, Ito Y, and Nakano H. Inhibitory effects of genistein on ATP-sensitive K^+ channels in rabbit portal vein smooth muscle. *Br J Pharmacol* 122: 1395–1404, 1997.

Palacios J, Marusic ET, Lopez NC, Gonzalez M, and Michea L. Estradiol-induced expression of N(+)-K(+)-ATPase catalytic isoforms in rat arteries: gender differences in activity mediated by nitric oxide donors. *Am J Physiol Heart Circ Physiol* 286: H1793–1800, 2004.

Pineda J, Kogan JH, and Aghajanian GK. Nitric oxide and carbon monoxide activate locus coeruleus neurons through a cGMP-dependent protein kinase: involvement of a nonselective cationic channel. *J Neurosci* 16: 1389–1399, 1996.

Pou S, Pou WS, Bredt DS, Snyder SH, and Rosen GM. Generation of superoxide by purified brain nitric oxide synthase. *J Biol Chem* 267: 24173–24176, 1992.

Prasad M and Goyal RK. Differential modulation of voltage-dependent K^+ currents in colonic smooth muscle by oxidants. *Am J Physiol Cell Physiol* 286: C671–C682, 2004.

Prast H and Philippu A. Nitric oxide as modulator of neuronal function. *Prog Neurobiol* 64: 51–68, 2001.

Safronov BV, Bischoff U, and Vogel W. Single voltage-gated K^+ channels and their functions in small dorsal root ganglion neurons of rat. *J Physiol* 493: 393–408, 1996.

Salter M, Knowles RG, and Moncada S. Widespread tissue distribution species distribution and changes in activity of Ca^{2+}-dependent and Ca^{2+}-independent nitric oxide synthase. *FEBS Lett* 291: 145–149, 1991.

Sheu FS, Zhu W, and Fung PC. Direct observation of trapping and release of nitric oxide by glutathione and cysteine with electron paramagnetic resonance spectroscopy. *Biophys J* 78: 1216–1226, 2000.

Shibuki K. An electrochemical microprobe for detecting nitric oxide release in brain tissue. *Neurosci Res* 9: 69–76, 1990.

Shinbo A and Iijima T. Potentiation by nitric oxide of the ATP-sensitive K^+ current induced by K^+ channel openers in guinea-pig ventricular cells. *Br J Pharmacol* 120: 1568–1574, 1997.

Stamler JS. Redox signaling: nitrosylation and related target interactions of nitric oxide. *Cell* 78: 931–936, 1994.

Stamler JS, Lamas S, and Fang FC. Nitrosylation. the prototypic redox-based signaling mechanism. *Cell* 106: 675–683, 2001.

Stamler JS, Simon DI, Osborne JA, Mullins ME, Jaraki O, Michel T, Singel DJ, and Loscalzo J. *S*-nitrosylation of proteins with nitric oxide: synthesis and characterization of biologically active compounds. *Proc Natl Acad Sci USA* 89: 444–448, 1992.

Stamler JS, Toone EJ, Lipton SA, and Sucher NJ. (S)NO signals: translocation, regulation, and a consensus motif. *Neuron* 18: 691–696, 1997.

Storm JF. Potassium currents in hippocampal pyramidial cells. *Prog Brain Res* 83: 161–187, 1990.

Surmeier DJ, Wilson CJ, and Eberwine J. Patch-clamp techniques for studying potassium currents in mammalian brain neurons. In: *Ion Channels of Excitable Cells*, edited by Narahashi T. San Diego, CA: Academic, 1994, p. 39–67.

Torphy TJ, Fine CF, Burman M, Barnette MS, and Ormsbee HS 3rd. Lower esophageal sphincter relaxation is associated with increased cyclic nucleotide content. *Am J Physiol Gastrointest Liver Phsiol* 251: G786–793, 1986.

Trapp S, Tucker SJ, and Ashcroft FM. Mechanism of ATP-sensitive K channel inhibition by sulfhydryl modification. *J Gen Physiol* 112: 325–332, 1998.

van der Vlies D, Pap EH, Post JA, Celis JE, and Wirtz KW. Endoplasmic reticulum resident proteins of normal human dermal fibroblasts are the major targets for oxidative stress induced by hydrogen peroxide. *Biochem J* 366: 825–830, 2002.

Waldron GJ and Cole WC. Activation of vascular smooth muscle K^+ channels by endothelium-derived relaxing factors. *Clin Exp Pharmacol Physiol* 26: 180–184, 1999.

White RE. Cyclic GMP and ion channel regulation. *Adv Second Messenger Phosphoprotein Res* 33: 251–277, 1999.

Xia R, Stangler T, and Abramson JJ. Skeletal muscle ryanodine receptor is a redox sensor with a well-defined redox potential that is sensitive to channel modulators. *J Biol Chem* 275: 36556–36561, 2000.

Xia Y, Dawson VL, Dawson TM, Snyder SH, and Zweier JL. Nitric oxide synthase generates superoxide and nitric oxide in arginine-depleted cells leading to peroxynitrite-mediated cellular injury. *Proc Natl Acad Sci USA* 93: 6770–6774, 1996.

Xu L Eu JP, Meissner G, and Stamler JS. Activation of the cardiac calcium release channel (ryanodine receptor) by poly-*S*-nitrosylation. *Science* 279: 234–237, 1998.

Yu SP, Yeh CH, Sensi SL, Gwag BJ, Canzoniero LM, Farhangrazi ZS, Ying HS, Tian M, Dugan LL, and Choi DW. Mediation of neuronal apotosis by enhancement of outward potassium current. *Science* 278: 114–117, 1997.

Yu SP, Farhangrazi ZS, Ying HS, Yeh CH, and Choi DW. Enhancement of outward potassium current may participate in beta-amyloid peptide-induced cortical neuronal death. *Neurobiol Dis* 5: 81–88, 1998.

Yue L, Feng J, Li GR, and Nattel S. Characterization of an ultrarapid delayed rectifier potassium channel involved in canine atrial repolarization. *J Physiol* 496: 647–662, 1996.

Zhou XB, Ruth P, Schlossmann J, Hofmann F, and Korth M. Protein phosphstase 2A is essential for the activation of Ca^{2+}-activated K^+ currents cGMP-dependent protein kinase in tracheal smooth muscle and Chinese hamster ovary cells. *J Biol Chem* 271: 19760–19767, 1996.